Journal of Bio- and Tribo-Corrosion (2020) 6:70
https://doi.org/10.1007/s40735-020-00362-x

Synergistic Study of Modified Sweet Potato Starch and KI for Corrosion Protection of Mild Steel in Acidic Media

C. K. Anyiam[1,3] · O. Ogbobe[2] · E. E. Oguzie[3] · I. C. Madufor[2]

Received: 27 July 2019 / Revised: 15 February 2020 / Accepted: 8 April 2020 / Published online: 30 April 2020

Abstract
Native starch (NS) extract from sweet potato was modified by alkaline treatment. The alkaline modified starch (AMS) and NS were characterized and assessed as corrosion inhibitor of mild steel under acidic conditions by gravimetric and potentiodynamic polarization techniques. Results obtained indicate that AMS exhibited higher inhibition efficacy that was stable over time. Synergistic use of potassium iodide improved the inhibitive efficacy of AMS. Polarization data propose that AMS operated via a mixed-inhibition mechanism and the experimental adsorption data followed Langmuir isotherm. The adsorption of AMS on the metals was established by Fourier transform infrared spectroscopy and Atomic force microscopy.

Keywords Mild steel · Sulphuric acid · FTIR · AFM · Biopolymers · Alkaline-modified starch

1 Introduction

The corrosion of metals and alloys remains a theme of intense economic and safety concerns. This is because metal and alloys are used to fabricate many engineering tools and component parts and some of these metallic materials are exposed to actions of acid during service. Hence, the exposure deteriorates the excellent properties of metal and alloys and poses great health-related challenges to man and his environment. Various methods have been employed in tackling the issue of corrosion, but the effective approach in combating corrosion in aqueous acidic environments remains the use of corrosion inhibitors. Corrosion inhibitors are often used to deter the attack of the acid solutions on metals in the course of acid pickling, oil well acidizing, acid cleaning, and industrial cleaning. They prevent corrosion by forming a protective layer when adsorbed on the surface of metals, which hinders access to corrodant [1–3].

✉ C. K. Anyiam
chokuim@yahoo.com

[1] Department of Prosthetics and Orthotics, Federal University of Technology, Owerri, Nigeria

[2] Department of Polymer and Textile Engineering, Federal University of Technology, Owerri, Nigeria

[3] Electrochemistry and Materials Science Research Laboratory, Department of Chemistry, Federal University of Technology, Owerri, Nigeria

A good corrosion inhibitor exhibits properties such as stability, economics, short- and long-term durability in service, safety, and hydrophobicity. Polymers due to their nature and functionality exhibit short- and long-term durability, impermeability to different media, innate stability, low cost, good chemical resistance and unusual deformation [4, 5].

Growing global concerns about the environment have in recent times promoted research efforts towards finding alternative low-toxicity polymeric corrosion inhibitors to replace synthetic polymeric corrosion inhibitors which in spite of their high efficiency are expensive, toxic and harmful [6].

Corrosion inhibitors derived from polymeric materials have drawn considerable attention in recent times due to their inherent stability, cost efficacy, unusual deformation, etc.[7–14]. Also, the formation of stable metal–polymer complexes on the metal surfaces is facilitated by the presence of surface active functional groups and unique electron delocalization [3, 15–17].

Biopolymers are a class of polymers that occur naturally and are thus environmentally friendly, cost-effective, with exceptional functionality and characteristics. They are extensively used in the construction and building, medical, biofuels, pharmaceutical, food preparation, cosmetics, paper, and textile industries. Interestingly, literature survey reveals that a number of naturally occurring bio-polymers such as cellulose, chitosan, chitin, tannic acid, lignin, starch, gums etc. have been used effectively for different corrosion control applications [3, 5, 7, 18–30]. Indeed, the molecular

structure of starch, a natural, renewable, and green polymer obtained from many plants, proposes that it has strong prospects to be an effective corrosion inhibitor. Moreover, it easily undergoes physical and chemical modifications, which allow modifications to the physical and chemical properties and hence its functionality [31–37].

A number of studies have focused on the corrosion inhibition performance of starches [23, 26, 38, 39]. Conversely, similar studies using modified starches [28, 33–36] are observed to exhibit improved inhibition efficacy. Therefore, it is the aim of this study to appraise the inhibitive efficacy of native sweet potato starch and modified sweet potato starch as corrosion inhibitors of mild steel in acid solution.

In this study, natural and modified sweet potato starch samples were prepared, characterized and subsequently investigated for corrosion protection efficacy on mild steel under acidic conditions using gravimetric and potentiodynamic polarization techniques. Also, the influence of iodide ions on the overall performance of the alkaline modified starch (AMS) was assessed. It is on record that synergistic effect ensues on addition of halide ions to organic compounds, which improves the effectiveness of corrosion protection [39–45]. Changes in the morphology of the corroding steel surface were studied by Fourier transform infrared spectroscopy and visualized by atomic force microscopy (AFM) respectively.

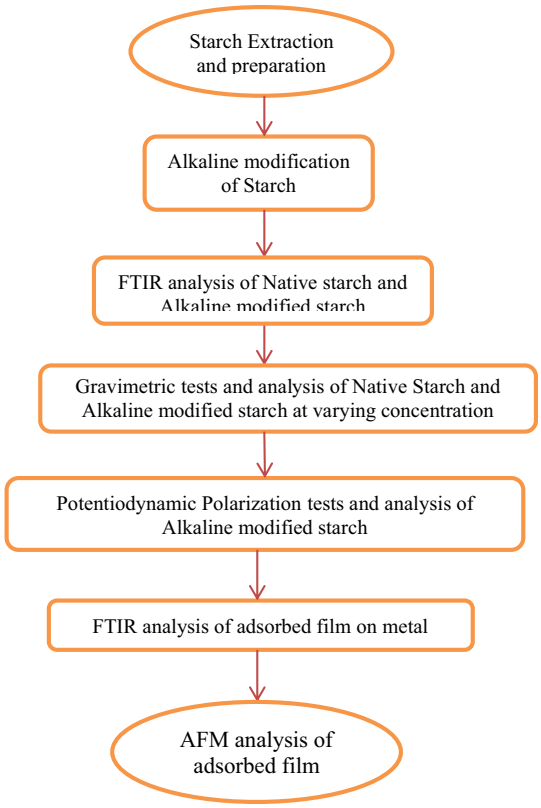

Fig. 1 Flow chart of the experimental program for the synergistic study of modified sweet potato starch and KI for corrosion protection of mild steel in acidic media

2 Experimental

2.1 Mild Steel Preparation

Mild steel specimens (C = 0.08 wt%, Si = 0.05 wt%, P = 1.00 wt%, Cu = 0.02 wt%, Pb = 0.02 wt% and Fe = 98.83 wt%) of dimensions of 30 × 30 × 10 mm were used for the gravimetric study and specimens with dimensions of 20 × 20 × 10 mm were used for potentiodynamic polarization studies. The mild steel surface was abraded to a fine finish and then cleaned with acetone and air-dried. The experimental procedure for the work is schematically presented in Fig. 1.

2.2 Preparation of Sweet Potato Starch

The sweet potato tubers (*Ipomoea batatas*) obtained from the local market were washed, peeled, chopped and blended with distilled water in a blender. An 80-mesh sieve was used to effect separation, the filtrate was left overnight at 15 °C, the supernatant was discarded and the precipitate collected. The re-suspension and sedimentation operation was reiterated until white starch was obtained. The sweet potato starch was dried at 50 °C for 6 h. The dried sweet potato starch was crushed and sieved through a 100-mesh sieve.

2.3 Alkaline Modification of Starch

The method of Chen and Jane [32] with minor adjustments was applied in the preparation of the AMS. 10 g of sweet potato starch was suspended in ethanol (40%) at 25 °C and stirred mechanically for 10 min. After which 12 g of NaOH was added at the rate of 4 g/min and mildly stirred for 15 min; subsequently ethanol (40%) was added slowly, with stirring for another 10 min. The slurry at 25 °C was left for 30 min to facilitate the settling of the treated sweet potato starch granules. The settled granules were washed with fresh ethanol solution, neutralized with 3 M HCl in absolute ethanol, and then rewashed with 60% and 95% ethanol solutions. The obtained starch was dehydrated with absolute ethanol, and finally oven-dried at 80 °C for 3 h to yield the AMS.

2.4 Gravimetric Measurement of Corrosion

The polished mild steel coupons of uniform size were weighed and suspended in 200 ml of the unstirred test solutions at room temperature (30 ± 10 °C). The test concentrations of the starch samples ranged from 0.1 to 0.7 g/l.

Weight loss was obtained relating to time, the coupons were retrieved from test solutions, cleaned, dried, and re-weighed singly at 24-h intervals progressively for 5 days. Weight loss was obtained from the difference between the weight of the coupon at a given time and its initial weight. All tests were run in triplicate and average values for each experiment obtained were used in subsequent calculations. The corrosion rate (CR) was obtained using Eq. 1

$$\mathrm{CR(mm/year)} = \frac{[\Delta W \times 87{,}600]}{\rho A t}, \tag{1}$$

where CR is the corrosion rate (mm/year), ΔW the change in weight (g), ρ the density of the coupon (g/cm^3), A the area of exposed surface of the coupon (cm^2) and t time of immersion (h). The percentage inhibitor efficiency (IE%) was calculated using Eq. 2 stated as follows:

$$\mathrm{IE\%} = \frac{\mathrm{CR_o} - \mathrm{CR_1}}{\mathrm{CR_o}} \times 100, \tag{2}$$

where $\mathrm{CR_o}$ is corrosion rate of mild steel in blank corrodent, and $\mathrm{CR_i}$ corrosion rate of mild steel in presence of the inhibitor.

2.5 Potentiodynamic Polarization Studies

The EG and G potentiostat/galvanostat, model 263A was used to carried out the potentiodynamic polarization studies. A corrosion cell from EG and G; model K0047 with Ag/AgCl electrode (saturated KCl) was used as the reference electrode, platinum wire as a counter electrode and mild steel coupons as the working electrodes. The tests were done at room temperature (30 ± 1 °C) using a scan rate of 0.166 mV/s, starting at a potential above 250 mV more active than the stable open circuit potential in the absence and presence of 0.5 g/l AMS and 0.5 g/l AMS + KI.

2.6 FTIR Studies

Fourier transform infrared (FTIR) spectra were obtained using a Nicolet Magna-IR 560 FTIR spectrophotometer at a frequency of 4000 to 400 cm^{-1}. The spectra for natural sweet potato starch and alkaline-modified potato starch (AMS) were obtained via the KBr pellet method. The corrosion product on mild steel surface immersed for 72 h in the acidic solution containing AMS was carefully scrapped off and the FTIR spectrum recorded.

2.7 AFM Surface Morphology Examination

The surface morphology of mild steel samples immersed in 0.25 M H_2SO_4 in the absence and presence of AMS for 6 and 24 h respectively was examined using the AFM (Agilent 5500 Scanning Probe Microscope). The Acoustic AC Mode (AAC Mode) with a cantilever oscillation frequency of 155 kHz was used to obtain the AFM images. The Picoscan Image 5 software was used to process the images.

3 Results and Discussion

3.1 FTIR Characterization of Unmodified and Modified Potato Starch

Figure 2 presents the FTIR spectra for native starch (NS) and AMS. The FTIR spectra of the NS showed complex vibrational modes owing to the pyranose ring of the glycosidic unit in regions below 800 cm^{-1} which is in line with the reports of Kizil and Seetharaman [33]. At the 1000–1200 cm^{-1} region, the common features of polysaccharides were observed, ring vibrations overlapped by broadening vibrations of C–OH side groups and the C–O–C glycosidic bond vibration [34]. The C–O and C–C stretching vibrations contribute to modes related to the bands at 994,

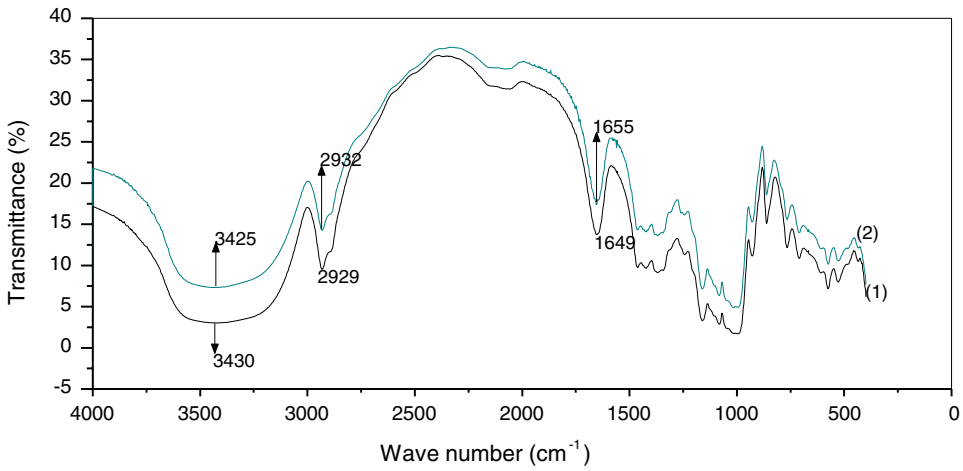

Fig. 2 FTIR spectra of sweet potato natural starch (1), and alkaline-treated starch (2)

1084, and 1163 cm^{-1} and the C–O–C glycosidic band at 860 cm^{-1}. Also, C–H bending are observed at bands 1465, 1425, and 1366 cm^{-1} as well as O–H bending and stretching bands at 1649 and 3430 cm^{-1}, which is ascribed to the complex vibrational stretches linked to the free, inter- and intra-molecular bound hydroxyl groups which constitutes the structure of starch [35]. Characteristic peaks were observed at 2929 cm^{-1} for C–H stretches related with the ring hydrogen atoms.

The FTIR spectrum of the AMS is also presented in Fig. 2 and reveals slight shifts in the positions of some peaks as well as increase in the intensity of some peaks. The major and strongest vibrational modes in the AMS spectrum are those located at 1016, 1026, 1158, 1371, 1422, 1655, and 2932, and a broad absorption band at 3000–3600 cm^{-1}. The strong vibrational mode positioned at 3000–3600 cm^{-1} is due to the stretching vibrations of the O–H bond, the vibrational mode located at 1016 cm^{-1} is attributed to the stretching vibrations of the C–O bond of carboxylate group associated with the AMS molecules, the two vibrational modes located at 1158, 1371 and 1422 cm^{-1}, with low intensity, could be assigned to the stretching vibrations of the C–O bond, and the weak vibrational mode located at 2932 cm^{-1} is ascribed to the stretching vibrations of the C–H bond. The relatively low-intensity absorption band located at 1655 cm^{-1} may be allotted to the stretching mode of carbonyl (C=O) group [33]. The narrowing of the O–H band at 3430 cm^{-1} as well as the sharper peak observed at 1649 cm^{-1} corresponds to loss of the bound water in starch due to the alkaline modification as observed by Fang et al. [35]. Starch is made up of a mixture of linear amylose and branched amylopectin chain, the anhydro-D-glucose units in amylopectin are linked through α-(1 → 6) glucosidic bonds whilst in amylose the anhydro-D-glucose units are linked through α-(1 → 4) glucosidic. During alkaline treatment, changes ensue in the amylose and amylopectin arrangements, and the amylose (which comprises the amorphous region) content is enriched due to the breaking down of α (1 → 6) bonds in the semi-crystalline amylopectin region. This is confirmed by the changes observed at the 1022 cm^{-1} wavelength, which denotes the starch amorphous region and 1044 cm^{-1} which represents the crystalline region of starch; this was observed by other researchers [31–37].

$$\text{Starch}-\text{OH} + \text{Na}-\text{OH} \rightarrow \text{Starch}-\text{OH} - \text{Na}^{-} + \text{H}_2\text{O}. \quad (3)$$

Also, when starch is treated with an alkali, it results in nucleophilic substitution as observed in the equation of reaction above which makes available the alkoxy groups (–CO^{-}) that are open for interaction. With the above findings, it could be inferred that alkaline treatment modifies the supermolecular structure of NS whilst the chemical structure is not significantly affected. This modification could be related to the narrowing of bands and increase in transmittance of the AMS spectra.

3.2 Corrosion Rates and Inhibition Efficiency

Figure 3a, b shows the trend of CRs of mild steel in 0.25 M H_2SO_4 in the absence and presence of NS and AMS, respectively. Results show that the CR was reduced in the presence of both NS and AMS, and this effect was enhanced with increasing starch concentration. This implies that both starches inhibited mild steel corrosion in 0.25 M H_2SO_4, in a concentration-dependent manner with CRs also decreasing with an increase in exposure time for all the systems. In inhibited solutions, it is assumed that corrosion is restricted to the unblocked sites left after some sites have been blocked by the adsorbed starch specie. Hence, the blocked sites have insignificant CRs and the degree of surface coverage relates to the CR with the expression.

$$\theta = 1 - \frac{\text{CR}_{\text{inh}}}{\text{CR}_{\text{o}}}. \quad (4)$$

Consequently, the reduction in CR by NS and AMS can be associated with the number of corrosion active sites that were blocked on the metal surface through adsorption; thus, the unblocked sites determine the CR [34].

Figure 3c, d shows the variation of inhibition efficiency of different concentrations of NS and AMS at different exposure intervals. Inhibition efficiency was enhanced as the concentration of NS and AMS was raised from 0.1 to 0.7 g/l, but decreased with an increase in immersion time.

In acidic solution, starch is partially hydrolyzed into simpler units by breaking down of the glucosidic bonds, resulting in solubilized starch granules that are of low viscosities, easily dispersible in solution, and readily adsorbed on the metal substrate.

It was observed that AMS exhibited higher inhibition efficacy which is associated to the active group present in the starch molecule; alkoxy (–CO−) groups facilitate active formation of an insoluble chelate with the ferrous cations generated during corrosion which seals the pores and flaws of the corrosion products' layer deposited onto the metal surface. This is in agreement with reports obtained from literature [23, 26, 28, 38, 39, 46].

Two important features can be deciphered from the trend of inhibition efficiency with AMS concentration and exposure time; inhibition efficacy clearly increased with the increase in AMS concentration but did not change significantly with exposure time. This implies that AMS maintained consistency in its corrosion protection action over time. Such stable and time-independent anticorrosion actions have significant implication in practical applications, by prolonging maintenance intervals. However, the maximum efficiency of AMS (62.8%) does not

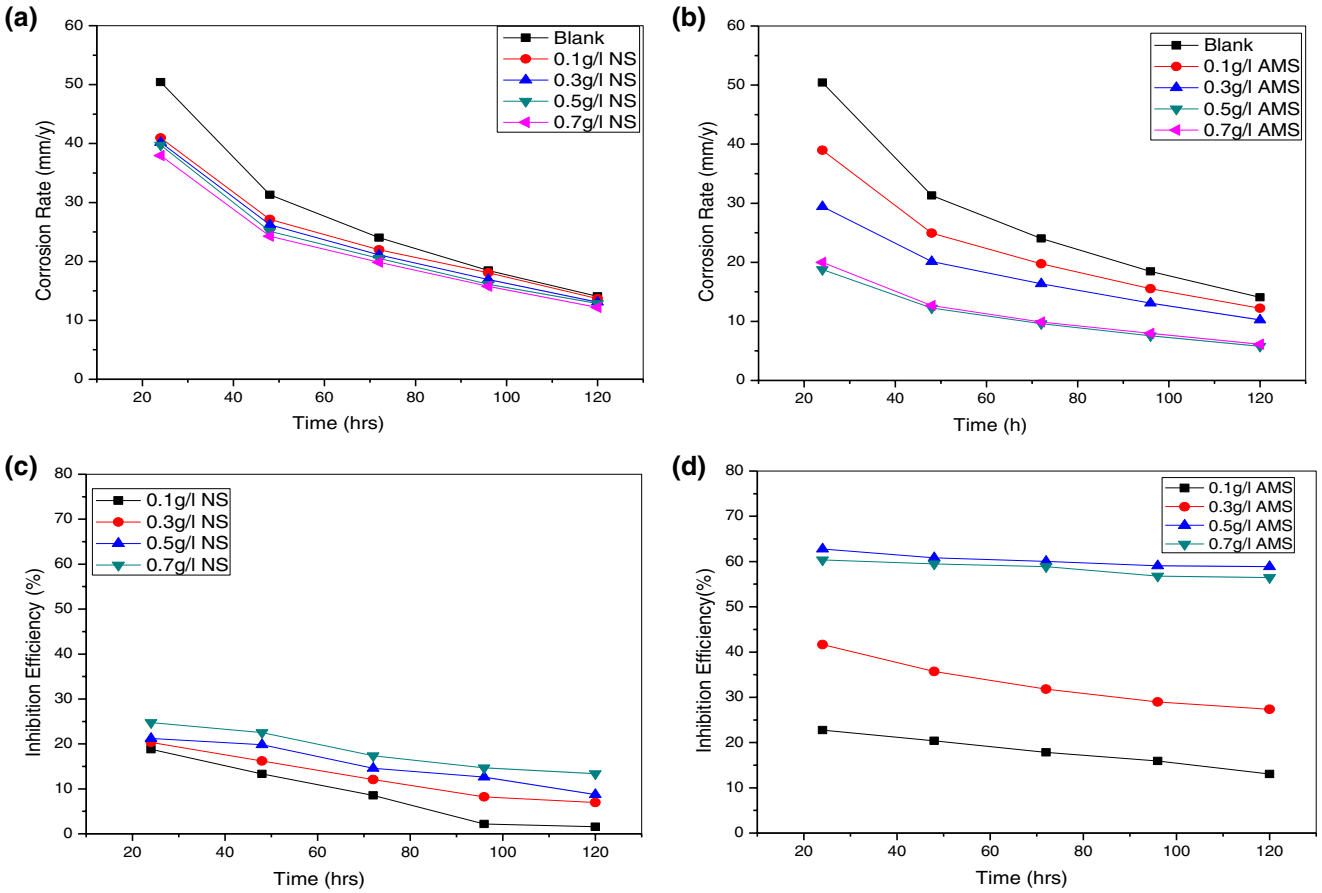

Fig. 3 Corrosion rate against time for mild steel in 0.25 M H_2SO_4 in the presence and absence of **a** natural starch, **b** alkaline-modified starch. Inhibition efficiency against time for mild steel in 0.25 M H_2SO_4 in the presence and absence of **c** natural starch, and **d** alkaline-modified starch

favourably recommend it for practical application, and hence there is the need to improve on inhibition efficiency possibly via synergistic interactions with other additives.

3.3 Synergistic Effects of Iodide Ions

The corrosion inhibition performance of some organic inhibitors has been enhanced by synergistic interactions with halide ions, especially iodide ions [40–45, 47, 48]. Recently, reports by researchers have tried to explain the mechanism of the synergistic effect and the general consensus is that halide ions increase the adsorption capacity of organic cations by forming interconnecting bridges between positively charged metal surface and inhibitor cations, which normally should repel each other [42–44, 49]. The dominant influence of the iodide ion ascribes to its large ionic radius, ease of polarizability and high hydrophobicity compared to bromide and chloride ions [42, 44].

$$Fe + H_2O + I^- \leftrightharpoons (FeIOH)^-_{ads} + H^+ + e, \quad (5a)$$

$$(FeIOH)^-_{ads} \rightarrow FeIOH + e, \quad (5b)$$

$$FeIOH + H^+ \leftrightharpoons Fe^{2+} + I^- + H_2O, \quad (5c)$$

where I represents the halide ion.

For the synergism experiments, AMS concentration of 0.5 g/l, being the most effective concentration from gravimetric experiments, was used, whilst KI concentration was 0.4 g/l. The effect of 0.4 g/l potassium iodide (KI) on the corrosion inhibition performance of 0.5 g/l AMS at different immersion periods improved synergistically. The result indicates clearly that the inhibition efficacy of the AMS + KI system reached 83% and maintained this value through all immersion periods. In other words, addition of the iodide ion synergistically improved the corrosion inhibition performance of AMS. The trend of IE% of AMS in combination with KI agrees well with that observed by Shaju and co-workers for the synergistic effect of KI on the corrosion inhibition efficiency of polynuclear Schiff bases, on mild steel in 0.5 M sulphuric acid as well as [45].

More importantly however is the fact that the AMS + KI couple maintained a steady value of inhibition efficiency for all immersion periods, just like was observed for AMS alone. This implies that the synergistic interactions yielded superior performance whilst maintaining the stable and time-independent anticorrosion action required for practical field applications.

3.4 Potentiodynamic Polarization Data

Potentiodynamic polarization measurements were carried out to obtain further insights on the inhibiting effect of AMS and AMS + KI from an electrochemical perspective. Polarization measurements are ideally appropriate for monitoring the effect of an additive on the kinetics and mechanisms of the anodic and cathodic partial reactions [50, 51]. The additives in this case were 0.5 g/l AMS as well as 0.5 g/l AMS + 0.4 g/l KI. The potentiodynamic polarization curves for the mild steel sample in 0.25 M H_2SO_4 without and with AMS and AMS + KI are presented in Fig. 4. The mild steel specimen exhibits active dissolution with no distinguishing transition to passivation within the potential range in all environments. The polarization curves show that AMS repressed the kinetics of both the anodic and cathodic reactions, reducing the corrosion current density (i_{corr}) from 294 to 103.9 A/cm^2, with further reduction to 46.48 A/cm^2 obtained for the AMS + KI system. The plots however reveal somewhat different mechanisms of action for AMS and AMS + KI. AMS caused a very slight shift of corrosion potential (E_{corr}) towards cathodic values and inhibited both the cathodic and anodic reactions, with a more pronounced cathodic effect on the cathodic hydrogen ion reduction reaction ($2H^+ + 2e \rightarrow H_2$). In other words, AMS functioned as a mixed-type inhibitor, with predominant cathodic effect.

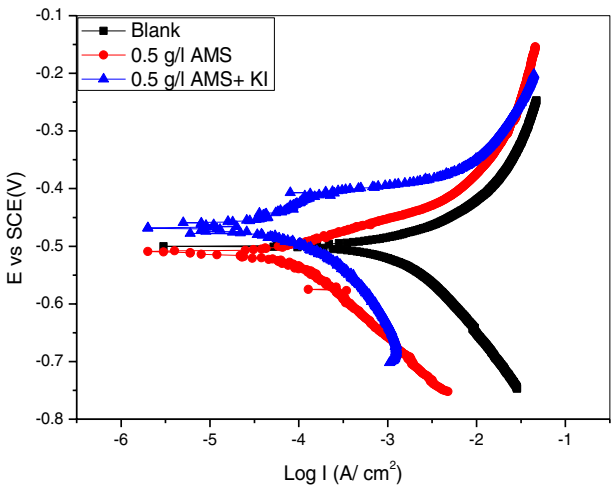

Fig. 4 Potentiodynamic polarization plots for mild steel in 0.25 M H_2SO_4 solution without and with AMS and AMS + KI

On the other hand, the AMS + KI couple caused an anodic (noble) shift in E_{corr}, which is the first pointer towards the superior anticorrosion performance of this system. The couple also functioned via a mixed inhibition mechanism, but in this case with a much more pronounced anodic effect. So, it appears that the primary role of the iodide ions was to enhance the inhibition of the anodic metal dissolution reaction ($Fe \rightarrow Fe + 2e$).

The corrosion current density values in the absence ($i_{corr,bl}$) and presence of inhibitor ($i_{corr,inh}$), obtained the from polarization data, were used to estimate the (IE_i%) using Eq. 7. The obtained values for the inhibition efficiency for AMS and AMS + KI are 64.2% and 84.2%, respectively.

$$IE\% = \left(1 - \frac{i_{corr,inh}}{i_{corr,bl}}\right) \times 100. \quad (6)$$

3.5 Adsorption Considerations

An inhibitor functions by a definite mechanism which is dependent on the electron density and polarizability of the functional group. Most organic inhibitors function by adsorption on the corroding metal surface and thereby restrict the ingress of corrodent species.

Surface coverage data (θ = IE/100) are very useful in determining the adsorption characteristics of an inhibitor. Such data are adapted in modelling corrosion inhibition data to adsorption isotherms which give in depth information on adsorption mechanisms. Accordingly, the surface coverage (θ) data obtained from gravimetric data for AMS were fitted to the Langmuir isotherm:

$$C/\theta = 1/b + C. \quad (7)$$

C is the inhibitor concentration and b is a constant. The plot of C/θ versus C is linear with a slope of 1.32, this suggests that the experimental data follow the Langmuir isotherm. Indeed, the corrosion inhibition and adsorption behaviour of a wide range of polymers have been described by the surface coverage data fit to various isotherms. Umoren [52] reported that inhibition process of guar gum on mild steel in acidic media was by chemical adsorption of the guar gum components onto mild steel surface following Temkin adsorption isotherm. In a related study of the corrosion inhibition of cast iron in acidic medium by glucose and hydroxylpropyl cellulose, Rajeswari (2013) observed that their mode of adsorption on the cast iron followed Langmuir adsorption isotherm [27]. Rosliza and Nik attributed the protection conferred by tapioca starch on AA6061 alloy surface to adsorption through all the functional groups present in the starch [26]. According to Solomon et al., the adsorption behaviour of carboxymethyl cellulose on mild steel in H_2SO_4

solution followed the Langmuir and Dubinin–Radushkevich adsorption isotherm models [21].

3.6 Analysis of the Adsorbed Inhibitor Film on Mild Steel

In the present study, FTIR spectra were used to support the fact that AMS functioned via adsorption on the mild steel surface. Presented in Fig. 5 are the FTIR spectra for the AMS starch sample and the inhibitor film scrapped off the surface of mild steel specimen immersed in 0.25 M H_2SO_4 containing AMS (Fe–AMS).

To address the adsorption of AMS onto the surface of mild steel and the possible formation of Fe–AMS complex, it is necessary to compare the relative intensities of the major vibrational modes of the AMS spectrum to those of the of Fe–AMS spectrum. It is clear that some peaks in the AMS sample are slightly present in the Fe–AMS complex. This confirms that some functional groups in the AMS sample are present in the adsorbed film. The strong C–O bond stretching frequency at 1158 cm^{-1}, slight stretches of C–H bond at 2932 cm^{-1}, and C=O bonds at 1655 cm^{-1} are present and shifted to lower frequency in the Fe–AMS complex spectrum. The changes in frequencies indicate that there is interaction between AMS and the surface of the metal [48]. The weak presence of some bonds in the Fe–AMS spectrum indicates that adsorption of AMS on mild steel surface might have ensued through these functional groups [53].

3.7 AFM Surface Morphological Studies

The surface morphology of the mild steel coupons was conducted by the AFM in the range 0 to 5000 nm at room temperature after immersion in blank solution and inhibited solutions for 3 h. The three-dimensional and two-dimensional surface images of the mild steel exposed to the free acid solution and inhibited acid solution are presented in Fig. 6a, b, c and d, respectively. Due to the absence of inhibitor there is rapid corrosion of the mild steel coupons as envisaged in Fig. 6a, rough surface characterized with gashes and deep ridges is observed. In the presence of AMS there is densification of the protective film of Fe^{2+}–AMS complex formed on the metal surface. The roughness results expressed as the root mean square roughness depict the standard deviation of the *Z* values (perpendicular to the *X*–*Y* plane) in a given area (scan area size analysed = 5 µm) and the mean roughness (Ra) which is the arithmetic averages of the deviations from the centre plane. The RMS for Fe^{2+}–AMS complex = 0.5 m/s on a scan area of 5 µm, whilst that of uninhibited metal = 1.0 m/s indicating a much rougher surface.

It is notable that the resultant amplitude image of AMS indicates large concentration of clusters that are dispersed consistently which is obvious in the low degree of dark on the colour scale as compared to the amplitude image of the uninhibited metal, which has little or no clusters and a high degree of dark on the colour scale. This is in agreement with the fundamentals of AFM which states, thus, imaging is sensitive to the chemical composition, viscoelasticity, and stiffness of a surface [54–56]. Thus, the observed colour scale on the images shows the existence of different materials on the surface of the metal, matching dark zones to the formation of a thin layer of corrosion products iron oxides and hydroxides and light zones to the presence of acid-modified starch molecules adsorbed on the metal surface.

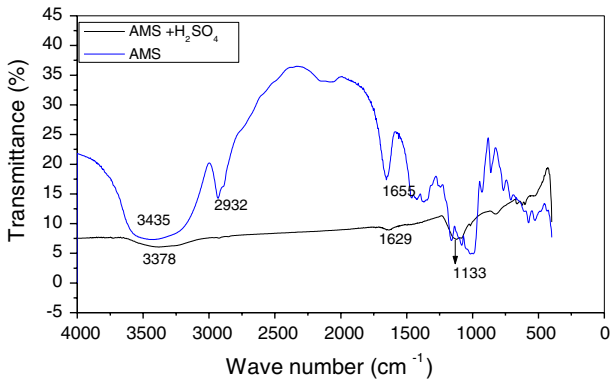

Fig. 5 FTIR spectra for AMS and AMS–mild steel complex in 0.25 M H_2SO_4 solution

4 Conclusion and Future Works

(i) Results obtained from FTIR analysis of native sweet potato starch (NS) and alkaline-modified sweet potato starch (AMS) confirmed the alkaline treatment of NS.

(ii) Gravimetric studies show that native sweet potato starch (NS) and alkaline-modified sweet potato starch (AMS) inhibited mild steel corrosion in 0.25 M H_2SO_4 solution with AMS exhibiting a higher inhibition efficacy.

(iii) The inhibition efficiency for both AMS and NS was found to increase as the inhibitor concentration increased but decreased with an increase in time of immersion. However, the inhibitive effect of AMS was observed to be stable over time and this could be ascribed to the bond between the mild steel surface and the active groups inherent in the AMS inhibitor.

(iv) The inhibition efficacy of the AMS inhibitor was synergistically enhanced by the addition of small amounts of KI.

(v) Polarization measurements obtained indicates that AMS inhibits corrosion through mixed inhibition

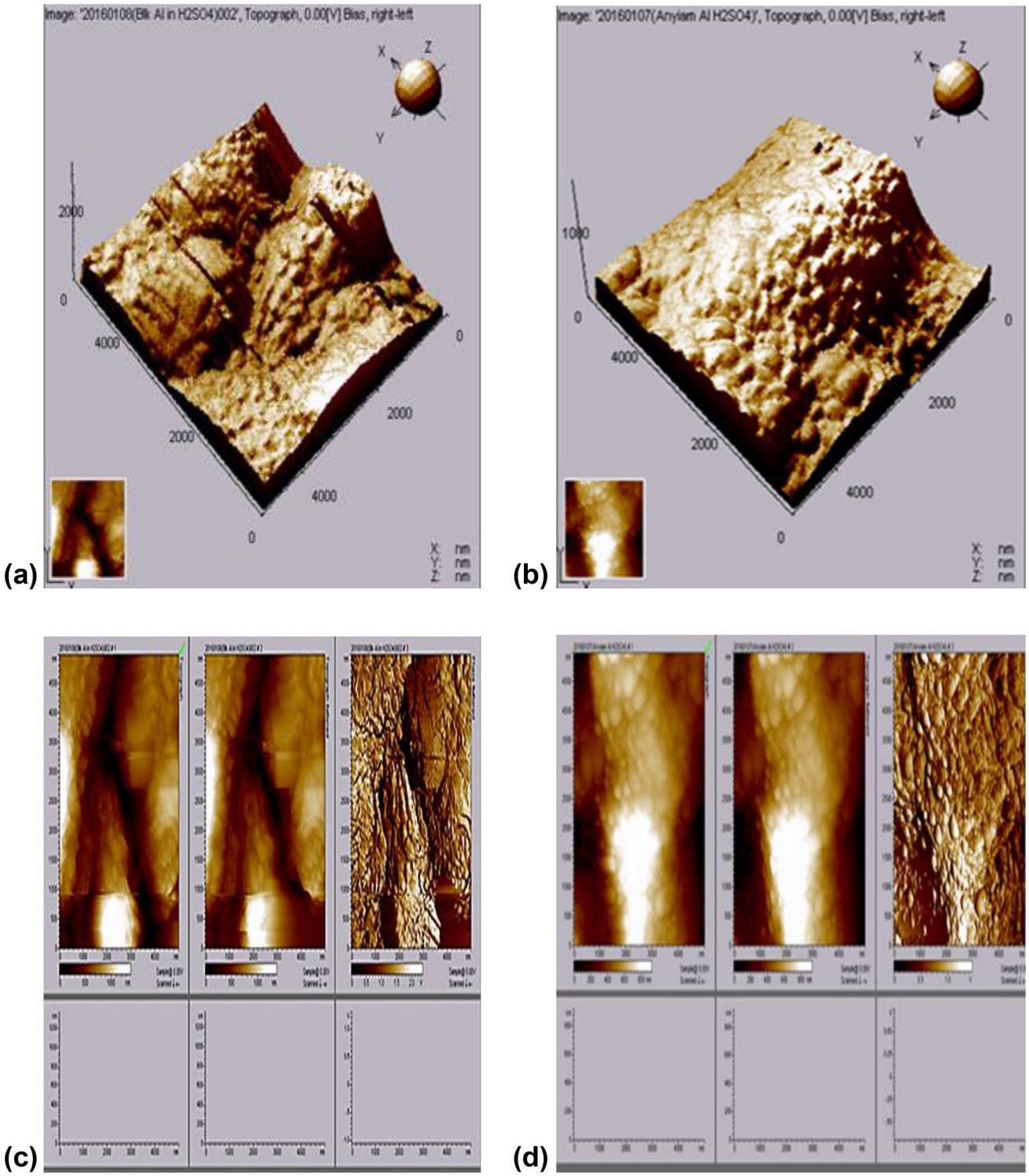

Fig. 6 AFM three-dimensional images for the mild steel surface in **a** blank 0.25 M H_2SO_4, **b** 0.25 M H_2SO_4 + 0.5 g/l AMS and two-dimensional images for the mild steel surface in **c** blank 0.25 M H_2SO_4, **d** 0.25 M H_2SO_4 + 0.5 g/l AMS

mechanism, with predominant cathodic effect. The AMS + KI couple exhibited a distinct anodic effect indicating the primary role of the iodide ions in promoting the inhibition of the anodic metal dissolution reaction.

(vi) The adsorption behaviour of AMS on the mild steel surface was estimated by the Langmuir isotherm.

(vii) The FTIR spectra and AFM images confirmed the adsorption of AMS molecules onto the mild steel substrate.

(viii) In future, our other works on the use of starch as a corrosion inhibitor should be geared towards modification of starch or blend to boost inhibition efficiency, improve stability and durability, and take adequate attention on application variations in different aggressive media.

Compliance with Ethical Standards

Conflict of interest The authors hereby declare that there were no conflict of interests regarding the publication of this paper.

References

1. Rajendran S, Sridevi SP, Anthony N, Amairaj AJ (2005) Corrosion behavior of carbon steel in polyvinyl alcohol. Anti-Corros Methods Mater 52:102–107
2. Oguzie EE (2008) Corrosion inhibitive effect and adsorption behaviour of *Hibiscus sabdaiffa* extract on mild steel in acid media. Port Electrochem Acta 26:303–314
3. Rani BEA, Basu BBJ (2012) Green inhibitors for corrosion protection of metals and alloys: an overview. Int J Corros 38:105–120
4. Yurt A, Butun V, Duran B (2007) Effect of the molecular weight and structure of some novel water soluble triblock copolymers on the electrochemical behaviour of mild steel. Mater Chem Phys 105:114–121
5. Umoren SA, Ebenso EE (2008) Blends of polyvinyl pyrrolidone and polyacrylamide as corrosion inhibitors for aluminium in acidic medium. Ind J Chem Technol 15:355–363
6. Palou RM, Olivares-Xomelt O, Likhanova NV (2010) Environmentally friendly corrosion inhibitors. InTech. https://doi.org/10.5772/57252
7. Umoren SA, Ebenso EE, Okafor PC, Ogbobe O (2006) Water soluble polymers as corrosion inhibitors of mild steel in acidic medium. Pigment Resin Technol 35:346–352
8. Pawar P, Gaikwad AB, Patil PP (2007) Corrosion by protective aspects of electrochemically synthesized poly(*o*-anisidine-*co*-otoluidine) coatings on copper. Port Electrochim Acta 52:5958–5967
9. Torresi RM, Solange S, Pereira da Silva JE, Susana T, Torresi C (2005) Galvanic coupling between metal substrate and polyaniline acrylic blends. Corrosion protection mechanism. Electrochim Acta 50:2213–2218
10. de Souza S (2007) Smart coating based on polyaniline acrylic blend for corrosion protection of different metals. Surf Coat Technol 201:7574–7581
11. Vera R, Schrebler R, Cury P, DelRio R (2007) Corrosion protection of carbon steel and copper by polyaniline and poly(*ortho*-methoxyaniline) films in sodium chloride medium. Electrochemical and morphological study. J Appl Electrochem 37:519–525
12. Umoren SA, Obot IB (2008) Polyvinyl pyrrolidone and polyacrylamide as corrosion inhibitors for mild steel in acidic medium. Surf Rev Lett 25:277–284
13. Devikala S, Kamaraj P, Arthanareeswari M (2014) PVD–TiO_2 composite as a corrosion inhibitor for mild steel in 3.5% NaCl. Int J Adv Chem Sci Appl 1(2):9–15
14. Umoren SA, Solomon MM (2014) Recent developments on the use of polymers as corrosion inhibitors—a review. Open Mater Sci J 8:39–54
15. Gandini A, Belgacem MN (2002) Recent contributions to the preparation of polymers derived from renewable resources. J Polym Environ 10:105–114
16. Ahmad S (2007) Polymer science, coatings and adhesives, safety aspects of coatings in coatings and adhesives. National Science Digital Library, NISCAIR, India
17. Metzger JO (2001) Organic reactions without organic solvents and oils and fats as renewable raw materials for the chemical industry. Chemosphere 43:83–87
18. Sugama T (1995) Pectin copolymers with organosiloxane grafts as corrosion-protective coatings for aluminium. Mater Lett 25:291–299
19. Raja PB, Sethuraman MG (2008) Natural products as corrosion inhibitor for metals in corrosive media—a review. Mater Lett 62:113–116
20. Ren Y, Luo Y, Zhang K, Zhu G, Tan X (2008) Lignin terpolymer for corrosion inhibition of mild steel in 10% hydrochloric acid medium. Corros Sci 50:3147–3153
21. Solomon MM, Umoren SA, Udosoro II, Udoh AP (2010) Inhibitive and adsorption behaviour of carboxymethyl cellulose on mild steel corrosion in sulphuric acid solution. Corros Sci 52:1317–1325
22. Oki M, Charles E, Alaka C, Oki TK (2011) Corrosion inhibition of mild steel in hydrochloric acid by tannins rom *Rhizophora racemosa*. Sci Res 2:6
23. Mobin M, Khan MA, Parveen M (2011) Inhibition of mild steel corrosion in acidic medium using starch and surfactants additives. J Appl Polym Sci 121:1558–1565
24. Sharmin E, Ahmad S, Zafar F (2012) Renewable resources in corrosion resistance. In: Shih H (ed) Corrosion resistance. InTech. www.intechopen.com/books/corrosion-resistance/renewable-resources-in-corrosion-resistance
25. Umoren SA, Banera MJ, Alonso-Garcia T, Gervasi CA, Mirifico MV (2013) Inhibition of mild steel corrosion in HCl solution using chitosan. Cellulose 20:2529–2545
26. Rosliza R, Wan Nik WB (2013) Improvement of corrosion resistance of AA6061 alloy by tapioca starch in seawater. Curr Appl Phys 10(1):221–229
27. Rajeswari V, Kesavan D, Gopiraman M, Viswanathamurthi P (2013) Physicochemical studies of glucose, gellan gum, and hydroxypropyl cellulose—inhibition of cast iron corrosion. Carbohydr Polym 95:288–294
28. Ochoa N, Marisela B, Sancristóbal IJ, Balsamo V, Albornoz A, Joaquin L et al (2013) Modified cassava starches as potential corrosion inhibitors for sustainable development. Mater Res 16:1209–1219
29. Ubong ME, Mazen MK (2014) Corrosion protection of steel sheets by chitosan from shrimp shells at acid pH. Cellulose 21:3139–3143
30. Umoren SA, Obot IB, Madhankumar A, Gasem ZM (2015) Performance evaluation of pectin as ecofriendly corrosion inhibitor for X60 pipeline steel in acid medium: experimental and theoretical approaches. Carbohydr Polym 125:280–291
31. Clerici MTPS (2012) Physical and/or chemical modifications of starch by thermoplastic extrusion, thermoplastic elastomers. https://www.intechopen.com/books/thermoplastic-elastomers/physical-and-or-chemical-modifications-of-starch-by-thermoplastic-extrusion
32. Chen J, Jane J (1994) Preparation of granular cold-water-soluble starches by alcoholic-alkaline treatment. Cereal Chem 71:618–622

33. Kizil J, Seetharaman K (2002) Characterization of irradiated starches by using FT-Raman and FTIR spectroscopy. J Agric Food Chem 50:3912
34. Mehdi JJ, Mohamadsaeed Y, Ashkan M (2014) Preparation of cold water-soluble potato starch and its characterization. J Food Sci Technol 51:601–605
35. Fang JM, Fowler PA, Sayers C, Williams PA (2004) The chemical modification of a range of starches under aqueous reaction condition. Carbohydr Polym 55:283–289
36. Han JA, Lim ST (2004) Structural changes in corn starches during alkaline dissolution by vortexing. Carbohydr Polym 55:193–199. https://doi.org/10.1016/j.carbpol.2003.09.006
37. Kaur B, Fazila A, Karim AA (2011) Alcoholic-alkaline treatment of sago starch and its effect on physicochemical properties. Food Bioprod Process 89:463–471. https://doi.org/10.1016/j.fbp.2010.09.003
38. Rosliza R (2012) Improvement of corrosion resistance of aluminium alloy by natural products. In: Shih H (ed) Corrosion resistance. InTech, pp 377–396. ISBN 978-953-51-0467-4
39. Nwanonenyi SC, Madufor IC, Uzoma PC, Chukwujike IC (2016) Corrosion inhibition of Mild Steel in sulphuric acid environment using millet starch and potassium. Int Res J Pure Appl Chem 12(2):1–15
40. Oguzie EE (2004) Influence of halide ions on the inhibitive effect of Congo red dye on the corrosion of mild steel in sulphuric acid solution. Mater Chem Phys 87:212–217
41. Oguzie EE, Unaegbu C, Ogukwe CN, Okolue BN, Onuchukwu AI (2004) Inhibition of mild steel corrosion in sulphuric acid using indigo dye and synergistic halide additives. Mater Chem Phys 84:363–368
42. Oguzie EE, Onuoha GN, Onuchukwu AI (2005) Inhibition of aluminium corrosion in potassium hydroxide by Congo red and its synergism with halide ions. Anti-Corros Methods Mater 52:293–299
43. Oguzie EE, Ebenso EE (2006) Studies on the corrosion inhibiting effect of Congo red dye-halide mixtures. Pigment Resin Technol 35:30–35
44. Oguzie EE, Li Y, Wang FH (2007) Corrosion inhibition and adsorption behavior of methionine on mild steel in sulfuric acid and synergistic effect of iodide ion. J Colloid Interface Sci 310:90–98
45. Umoren SA, Solomon MM (2010) Effect of halide ions additives on the corrosion inhibition of aluminum in HCl by polyacrylamide. Arab J Sci Eng 35:115–129
46. Li X, Deng S, Lin T, Xie X, Du G (2019) Cassava starch ternary graft copolymer as a corrosion inhibitor for steel in HCl solution. J Mater Res Technol. https://doi.org/10.1016/j.jmrt.2019.12.050
47. Suzuki T, Nishihara H, Aramaki K (1996) The synergistic inhibition effect of octylmercaptopropionate and 8-quinolinol on the corrosion of iron in an aerated 0.5 M Na_2SO_4 solution. Corros Sci 38:1223–1234
48. Eddy NO, Ebenso EE (2010) Adsorption and quantum chemical studies on cloxacillin and halides for the corrosion of mild steel in acidic medium. Int J Electrochem Sci 5:731–750
49. Shaju KS, Thomas KJ, Vinod PR, Aby P (2012) Synergistic effect of KI on corrosion inhibition of mild steel by polynuclear Schiff base in sulphuric acid. Hindawi. https://doi.org/10.5402/2012/425878
50. Li XH, Deng SD, Fu H, Li YX (2017) Corrosion inhibition of cationic cassava starch graft copolymer for steel in HCl solution. Fine Chem 34:319–325
51. Li X, Deng S, Lin T, Xie X, Du G (2018) Cassava starch sodium allylsulfonate acryl amide graft copolymer as an effective inhibitor of aluminium corrosion in HCl solution. J Taiwan Inst Chem Eng 86:252–269
52. Umoren SA (2008) Inhibition of aluminium and mild steel corrosion in acidic medium using gum Arabic. Cellulose 15:751–761
53. Eddy NO, Odiongenyi AO (2010) Corrosion inhibition and adsorption properties of ethanol extract of *Heinsia crinata* on mild steel in H_2SO_4. Pigment Resin Technol 38:288
54. Braga PC, Ricci D (2004) Imaging methods in atomic force microscopy. In: Methods in molecular biology. Humana Press, Totowa, pp 13–23
55. Yu JJ, Magonov SN (2007) Application of atomic force microscopy (AFM) in polymeric materials. Application note. Agilent Technologies, Inc., Santa Clara
56. Bello M, Ochoa N, Balsamo V, López-Carrasquero F, Coll S, Monsalve A et al (2010) Modified cassava starches as green corrosion inhibitors of carbon steel: an electrochemical and morphological approach. Carbohydr Polym 82:561–568. https://doi.org/10.1016/j.carbpol.2010.05.019